Coal Conversion Wastewater Treatment by Cataltyic Oxidation in Supercritical Water

Semi-Annual Report
January 1 - June 30, 1997

By
Phillip E. Savage

By
University of Michigan

Disclaimer

DISCLAIMER

Portions of this document may be illegible
in electronic image products. Images are
produced from the best available original
document.

Introduction

In previous reports, we showed that CARULITE 150 from Carus Chemical Company was so effective with oxidation of phenol in supercritical water (SCW) that the results we obtained were likely influenced by internal mass-transfer resistance. We also reported that oxidation of phenol over MnO_2 powder in SCW improved the conversions of both phenol and total organic carbon (TOC) relative to non-catalytic oxidation while the catalytic oxidation kinetics was free from mass-transfer limitation. In this report we continued the investigation of oxidation over the MnO_2 powder in SCW.

Experimental Section

Phenol oxidation experiments were performed in isothermal, tubular reactors at 380 °C and 250 atm, using a design identical to used in previous non-catalytic supercritical water oxidation (SCWO) experiments except that MnO_2 particles (125 ~ 250 μm in diameter) were placed inside the reactor. High pressure pumps deliver two streams containing the phenol and H_2O_2 aqueous solutions, which are preheated separately in two 1/16-in. (1.6-mm) OD feed lines before being mixed in a Hastelloy C-276 cross. The reactor was constructed of 1/4-in. (6.4-mm) OD Hastelloy C-276 tubing and had a length between 4.6 and 10.7 cm. It was connected to the mixing cross and separation part by a 1/8-in. (3.2-mm) OD line and a 1/16-in. OD line, respectively. The lines joined the tubular reactor through two stainless steel reducing unions made by Swagelok, and two porous Hastelloy disks (100 μm opening) are placed at the ends of the reactor to hold the catalyst inside. The reactor assembly is housed in a temperature-controlled fluidized sand bath that maintains isothermality to within 1 °C. Upon leaving the heated zone of the

sand bath, the reactor effluent is cooled and then depressurized and separated into vapor and liquid fractions.

Unreacted phenol in the reactor effluent is quantified to within 2% using reversed-phase, isocratic, high-performance liquid chromatograph (HPLC). We used a C18 column, a mobile phase of acetonitrile and water (28:72 by volume) and UV detection at 210 nm. Quantification of CO_2 and CO is accomplished with an on-line gas chromatograph with thermal conductivity detector (GC-TCD).

Results and Discussion

We continued our investigation of SCWO of phenol over MnO_2 powder at 380 °C and 250 atm. The amount of unsupported catalyst ranged from 1.60 to 3.77 g. A total of 46 reactions were run, which are summarized in Tables 1. Phenol conversions from 56% to 100% were obtained at the space time of 7.5 to 38.4 second. By contrast, the phenol conversions calculated from the non-catalytic oxidation under the identical conditions (same temperature, pressure, concentrations of reactants, and reactor, but without catalyst) were between 6.1% to 27.3% (1). So under these conditions even the MnO_2 itself is effective enough to improve the kinetics substantially compared to non-catalytic oxidation.

Since the phenol conversions were still high (most of them over 80%), these data are not adequate for establishment of the global rate law for phenol conversion. On the contrary, a wide range of CO_2 yields was obtained, from 10.5% to 71.6%. The non-catalytic CO_2 yield was calculated to range from 1.6% to 11.6% (2). These results show that the MnO_2 powder improved the complete oxidation to CO_2 compared to that of non-catalytic oxidation, but by much less than the CARULITE 150 catalyst.

Table 1. Phenol oxidation over MnO_2 powder at 380 °C and 250 atm

| Space time (s)	[PhOH] (M)	[O_2] (M)	Measured conversion	CO_2 yield	Calc. CO_2 yield	Residence time (s)	Calc. non-cat. conversion	Calc. non-cat. CO_2 yield
31.32	3.97E-04	4.01E-02	0.970	0.716	0.734	5.39	0.188	0.073
23.89	6.49E-04	3.76E-02	0.963	0.504	0.528	5.06	0.165	0.060
14.63	6.40E-04	5.03E-02	0.967	0.455	0.360	6.03	0.214	0.087
19.92	6.05E-04	5.29E-02	0.973	0.625	0.476	3.53	0.135	0.054
32.37	1.09E-03	6.45E-02	0.987	0.604	0.589	6.68	0.253	0.104
38.43	1.20E-03	7.12E-02	0.981	0.444	0.652	4.63	0.186	0.077
20.19	7.59E-04	9.96E-02	0.986	0.457	0.466	4.77	0.234	0.108
14.89	1.20E-03	7.03E-02	0.966	0.345	0.302	3.37	0.138	0.056
38.55	9.33E-04	6.27E-02	0.974	0.466	0.693	7.28	0.273	0.114
16.98	1.01E-03	6.20E-02	0.920	0.341	0.356	3.30	0.132	0.052
13.09	1.30E-03	4.83E-02	0.835	0.175	0.255	2.57	0.089	0.033
10.54	1.13E-03	6.88E-02	0.936	0.289	0.225	2.18	0.092	0.036
9.63	1.32E-03	6.71E-02	0.852	0.142	0.195	2.12	0.086	0.034
11.89	4.75E-04	1.09E-01	0.937	0.334	0.349	2.53	0.149	0.068
9.51	8.83E-04	8.88E-02	0.934	0.238	0.227	2.05	0.101	0.043
30.22	9.33E-04	7.40E-02	0.977	0.569	0.589	6.25	0.259	0.110
31.02	8.95E-04	7.58E-02	0.972	0.590	0.609	6.40	0.269	0.116
18.99	1.47E-03	4.75E-02	0.877	0.293	0.340	4.02	0.133	0.049
13.60	1.07E-03	6.56E-02	0.930	0.373	0.288	2.79	0.115	0.045
12.73	1.19E-03	6.37E-02	0.844	0.260	0.261	2.71	0.108	0.042
13.24	1.12E-03	6.51E-02	0.897	0.287	0.276	2.77	0.113	0.044
8.36	1.22E-03	6.89E-02	0.918	0.297	0.176	1.88	0.078	0.031
7.51	9.70E-04	8.38E-02	0.923	0.245	0.175	1.70	0.081	0.034
32.02	9.18E-04	4.79E-02	0.985	0.590	0.603	6.51	0.222	0.085
30.54	9.84E-04	4.59E-02	0.983	0.582	0.569	6.23	0.207	0.079
22.35	1.33E-03	3.37E-02	0.923	0.373	0.395	4.57	0.129	0.045
18.43	1.51E-03	2.80E-02	0.870	0.251	0.317	3.80	0.098	0.032
21.02	3.72E-04	6.70E-02	1.000	0.629	0.583	4.25	0.198	0.084
13.50	1.07E-03	4.41E-02	0.946	0.458	0.279	2.80	0.095	0.035
11.84	6.38E-04	6.12E-02	0.938	0.439	0.303	2.51	0.108	0.043
8.38	1.19E-03	4.50E-02	0.855	0.245	0.173	1.84	0.063	0.023
10.46	3.06E-04	7.27E-02	0.953	0.465	0.353	2.20	0.115	0.048
9.43	4.99E-04	6.47E-02	0.911	0.354	0.270	1.96	0.091	0.036
8.46	7.10E-04	6.01E-02	0.859	0.186	0.215	1.82	0.077	0.030
32.39	8.35E-04	4.72E-02	0.960	0.433	0.624	6.26	0.215	0.083
31.38	1.74E-03	4.50E-02	0.945	0.463	0.489	5.96	0.181	0.067
22.35	2.50E-03	3.24E-02	0.744	0.258	0.319	4.30	0.109	0.037
18.47	1.17E-03	2.72E-02	0.962	0.431	0.345	3.61	0.095	0.031
14.98	1.78E-03	4.93E-02	0.896	0.487	0.258	3.03	0.101	0.037
15.92	1.59E-03	5.20E-02	0.853	0.336	0.285	3.20	0.110	0.041
31.49	1.97E-03	1.81E-02	0.776	0.265	0.446	6.06	0.118	0.036
33.45	1.79E-03	1.89E-02	0.771	0.244	0.484	6.33	0.127	0.039
27.35	2.25E-03	1.55E-02	0.714	0.180	0.376	5.20	0.093	0.027
23.97	1.29E-03	2.31E-02	0.750	0.293	0.413	4.58	0.108	0.034
15.69	2.38E-03	1.54E-02	0.560	0.105	0.224	3.06	0.055	0.016
15.06	1.78E-03	1.93E-02	0.599	0.187	0.243	2.88	0.061	0.018
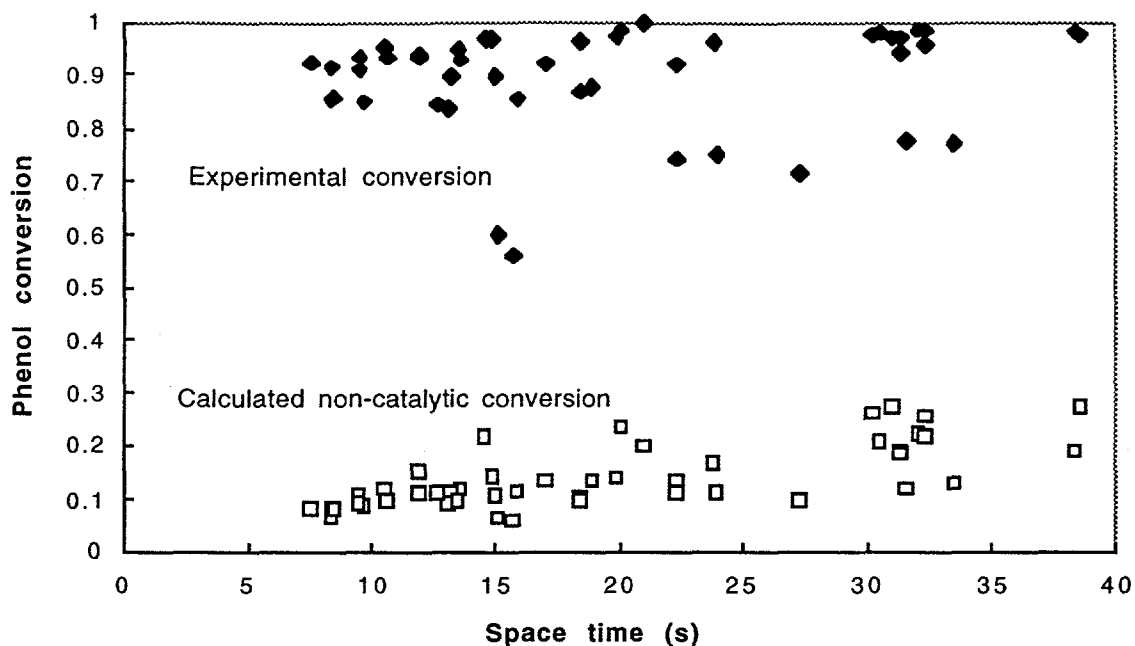
Figure 1. Experimental phenol conversions over bulk MnO_2 compared with the calculated non-catalytic phenol conversions.

Figures 1 and 2 provide comparisons of the phenol conversions (X_p) and the CO_2 yields (X_c) experimentally observed and calculated for non-catalytic SCWO under identical conditions. While the unsupported MnO_2 improved both phenol conversion and CO_2 formation substantially, the effect of this unsupported catalyst is much less dramatic than that of the CARULITE 150. Note these data were collected with space times up to 40 seconds. For SCWO of phenol over the CARULITE 150 complete oxidation to CO_2 is achieved in several seconds of space time.
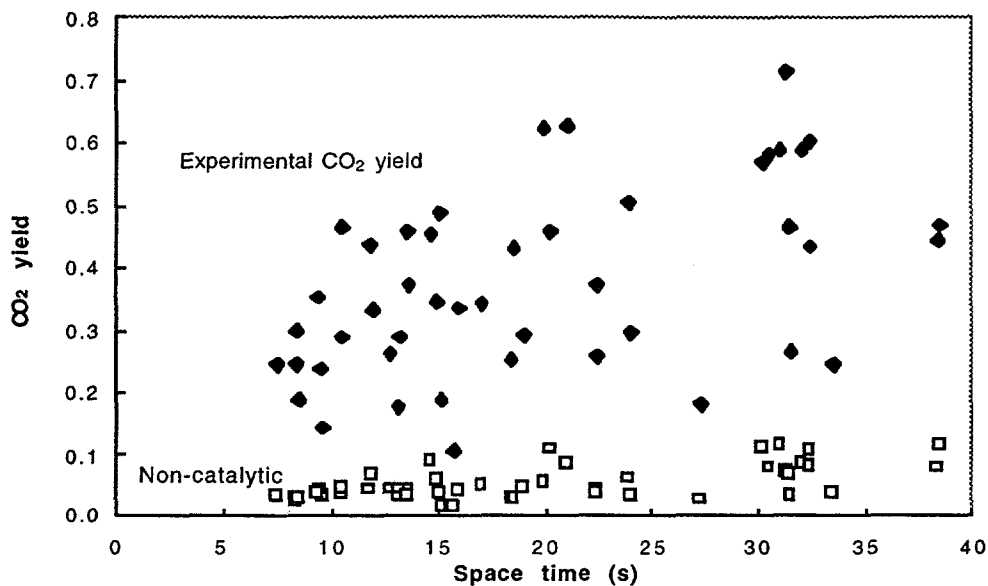
Figure 2. Experimental CO_2 yields from phenol oxidation over bulk MnO_2 compared with the calculated non-catalytic CO_2 yields.

The objective of our CO_2 formation global kinetics analysis was to determine the Arrhenius parameters for the reaction rate constant and the reaction orders. Since the data collected so far were at the same temperature and pressure, we are not able to estimate the Arrhenius parameters and the reaction order in water concentration. Instead, the following power-law rate expression is used:

$$\text{rate of } CO_2 \text{ formation} = k[TOC]^a[O_2]^b$$

Power-law rate expressions have been used frequently to correlate the global kinetics of both reactant disappearance and CO_2 formation for non-catalytic SCWO (1, 2). They typically capture the general trends in the experimental data, but cannot be expected to model the details of the complex oxidation chemistry. Although the catalytic kinetics are expected to be quite different from those of non-catalytic SCWO, we will use the power-law expressions in this preliminary analysis. TOC is defined as carbon contained in all compounds that can be further oxidized to CO_2. Thus, the rate of TOC disappearance is the same as the rate of CO_2 formation. By combining the design equation (3) for the isobaric, isothermal, plug-flow reactor with the power-law rate we obtain:

$$\frac{dX_c}{d\tau'} = 1000\rho k[TOC]_o^{a-1}[O_2]^b(1-X_c)$$

Most of the reactions listed in Table 1 were run with large excess amount of initial O_2 concentrations. Only the last 6 reactions (at the bottom in Table 1) did not have large excess amount of O_2. All but two among the rest were conducted with at least 230% excess amount of O_2. For a reaction with a large excess amount of oxygen, the oxygen concentrations could be approximated as being roughly equal to its initial concentration. The differential equation above now can be solved analytically with the initial condition $X_c = 0$ at $\tau' = 0$ to give:

$$(1-X_c)^{1-a} = 1-1000(1-a)\rho k[TOC]_o^{a-1}[O_2]_o^b\tau'$$

when a does not equal to 1. Optimized values for the parameters k, a and b with the 95% confidence intervals were determined by applying nonlinear

6

regression techniques. The rate law of TOC destruction for the reactions with large excess amount of oxygen was determined as:

$$\text{rate of CO}_2 \text{ formation} = 10^{2.20 \pm 0.72}[TOC]^{0.61 \pm 0.20}[O_2]^{0.08 \pm 0.32}$$

Figure 3 compares the experimental CO_2 yields and calculated values on the basis of this rate law, which gives a fair match. The calculated CO_2 yields (including those with little excess oxygen) are also included in Table 1.

The reaction order for the organic carbon here is slightly smaller than the value of 0.82 determined for the non-catalytic TOC destruction rate during SCWO of phenol. The most remarkable difference between the catalytic and non-catalytic rate laws, however, is the reaction order for oxygen is about 0, while that of the non-catalytic SCWO is 0.71. This difference implies that the reaction pathway, mechanism and rate law for the catalytic oxidation may be quite different from those of non-catalytic oxidation. For example, the rate law in the Langmuir-Hinshelwood form (3) may be a better model for catalytic SCWO.
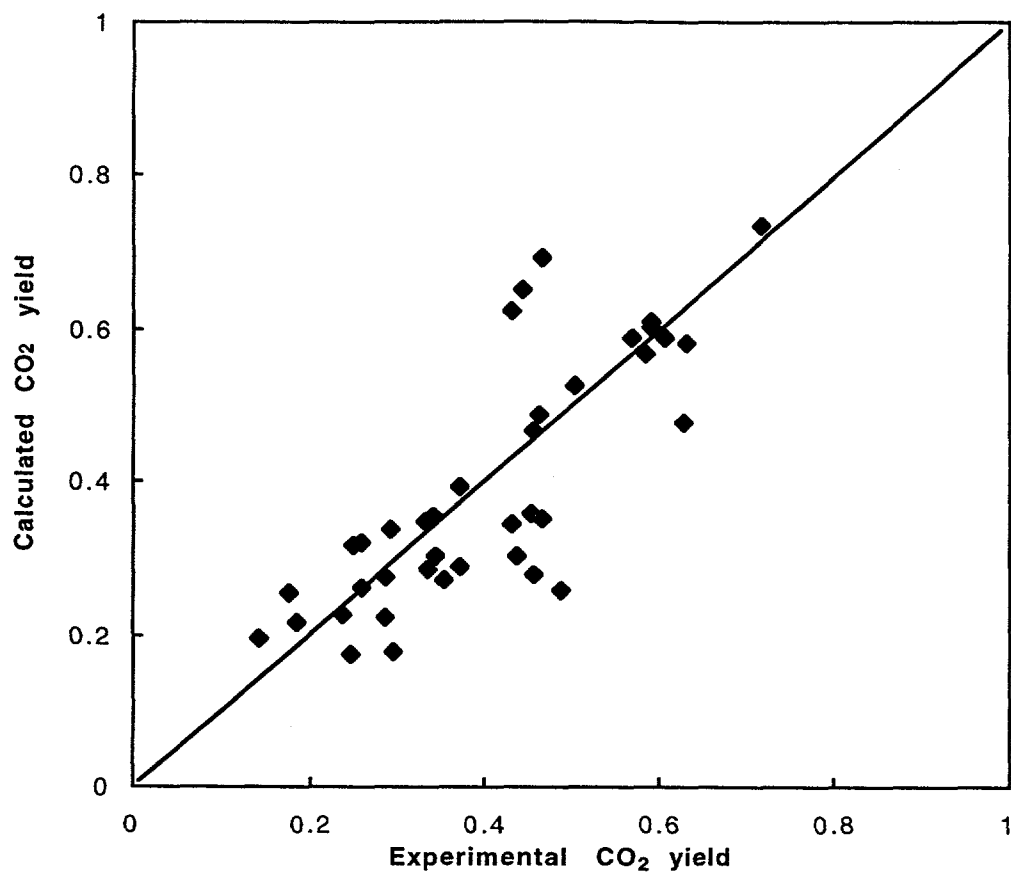
Figure 3. Comparison of experimental and calculated TOC conversions for phenol oxidation in SCW over bulk MnO_2.

Conclusion

Oxidation of phenol over the MnO_2 powder improves the oxidation rate up to an order of magnitude under the conditions taken here relative to that of the non-catalytic SCWO. At 380 °C and 250 atm, the rate of TOC destruction is found to have reaction orders of 0.61 ± 0.20 in the organic carbon and 0.08 ± 0.32 in oxygen.

Future Plans

We will continue the investigation SCWO of phenol over the MnO_2 powder at different temperatures and pressures to establish the full kinetics for both phenol and TOC disappearance.

We will also investigate SCWO of phenol over the supported MnO_2 catalyst like CARULITE 150. We will do so after eliminating the internal mass-transfer resistance, and studying the stability and durability of the supported catalyst. Eventually we will correlate the studies on both unsupported and supported catalysts.

Notation

a = reaction order for the organic carbon

b = reaction order for the oxygen

k = rate constant

ρ = fluid density, g/cm^3

τ' = space time: ratio of catalyst weight to mass flow rate, s

τ = residence time: ratio of reactor volume to volume flow rate, s

X_p = conversion of phenol

X_c = conversion of TOC or CO_2 yield

Literature References

1. Gopalan, S., Savage, P. E. *AICHE J.* **1995**, *41*, 1864.

2. Li, R.; Thornton, T. D.; Savage, P. E. *Environ. Sci. Technol.* **1992**, *26*, 2388.

3. Fogler, H. S. Elements of Chemical Reaction Engineering, second Ed., PRENTICE HALL, New Jersey, 1992.